


A Location-Aware and Greedy Cross-Layer Routing Protocol for Flying Ad-hoc Networks

Rian T. D. Moreira  [Universidade Federal Fluminense | riandias@id.uff.br]

Dianne S. V. Medeiros   [Universidade Federal Fluminense | diannescherly@id.uff.br]

 Telecommunications Engineering Department, Universidade Federal Fluminense, 156, Passo da Pátria street, Praia Vermelha Campus, São Domingos, Niterói, RJ, 24210-240, Brazil.

Received: 26 February 2024 • **Accepted:** 11 November 2024 • **Published:** 22 December 2024

Abstract The Flying *Ad-hoc* Networks (FANETs) enhance the coverage capacity in cellular networks by forwarding data in multiple hops using Unmanned Aerial Vehicles (UAVs). Nevertheless, unlike classic *ad-hoc* networks, FANETs have specific characteristics, such as free movement in three dimensions and very high-speed nodes. These characteristics lead to a more complex and dynamic mobility pattern compared to other *ad-hoc* networks, generating more frequent topology changes. This paper proposes the Greedy Weighted Perimeter Routing Protocol (GWPRP), which aims to improve networking performance. GWPRP is a location-aware and greedy cross-layer routing protocol based on a classic protocol for vehicular networks, the Greedy Perimeter Stateless Routing (GPSR). Following a similar greedy strategy, GWPRP forwards packets based only on local information obtained from neighbors, which considers link and network layer information, local link stability, and node location. We assess the protocol in a simulated environment, comparing its performance with GPSR and Energy Efficient Hello *Ad-hoc* On-Demand Distance Vector (EE HELLO AODV), a variant of AODV for FANETs. The results show that GWPRP achieves a higher packet delivery ratio with smaller control overhead and lower average end-to-end delay and jitter.

Keywords: FANET, Routing, Forwarding, Greedy, Cross-layer

1 Introduction

Although Unmanned Aerial Vehicles (UAVs) have been used in military applications for decades, their application in civilian scenarios has only recently gained popularity [Mahmud and Cho, 2019]. Current civilian applications include but are not limited to searching and rescuing operations, monitoring regions with security cameras, sensing temperature, humidity, and pollution levels in an area, signal coverage in a region, and data routing. The deployment of the 5th Generation (5G) cellular mobile network also promotes the use of UAVs, with the primary goal of temporarily expanding the network coverage area. In this scenario, the UAVs form a Flying *Ad-hoc* Network (FANET) to cover a shadowed region by transferring information through multiple hops via several UAVs to a base station [Khan *et al.*, 2021].

FANETs differ from classic Mobile *Ad-hoc* Networks (MANETs) and Vehicle *Ad-hoc* Networks (VANETs) mainly due to the topology dynamics and the energetic constraints. Node speed in FANETs can vary between 30 and 460 km/h [Khan *et al.*, 2019], much higher than in MANETs and typical VANETs. Moreover, nodes can move in a three-dimensional space in FANETs, not restricted to roads. Node mobility is also prone to unexpected changes due to the influence of meteorological conditions, such as high-speed wind. Additionally, computing and energy constraints pose challenges for maintaining FANETs operation over an extended period [Ashish and Jay, 2021]. These characteristics make standards and protocols for VANETs and MANETs obsolete for FANETs. Thus, there is an opportunity for developing novel communication protocols for FANETs, which

must consider the three-dimensional dynamics of network elements and UAV constraints [A. Chrikiac and Kamoun, 2019].

This paper proposes the Greedy Weighted Perimeter Routing Protocol (GWPRP), a new cross-layer routing protocol for FANETs that applies a greedy forwarding strategy based on the nodes' geographic location and characteristics of the link and network layers to determine the best neighbor toward the destination. GWPRP is based on the Greedy Perimeter Stateless Routing (GPSR), but the proposed protocol modifies GPSR's control messages to consider the third dimension, to include information about the link layer, such as the Frame Error Rate (FER) of each neighbor, and to include information about the network layer, such as the number of packets in the transmission queue of neighboring nodes. Moreover, GWPRP assigns a stability level to 1-hop neighbors based on the consecutive control messages received from the neighbor. This information is also used in the forwarding decision-making process.

GWPRP is assessed through comparative simulations using the Network Simulator 3 (NS-3), version 3.29. The evaluated scenario considers UAVs randomly distributed in a region shaped like a cube and UAVs moving randomly with a constant random speed within this region. GWPRP is compared to the Energy Efficient Hello *Ad-hoc* On-Demand Distance Vector (EE HELLO AODV) [Mahmud and Cho, 2019], a protocol based on AODV but created for FANETs, and GPSR [Karp and Kung, 2000], one of the well-known location-based protocols in the literature. As such, the evaluation considers GPSR's performance as the baseline for location-based protocols. In turn, EE HELLO AODV rep-

resents energy-efficient protocols that focus specifically on FANETs. Moreover, these protocols have public standard implementations. The results show that GWPRP achieves the highest packet delivery rate, with lower average end-to-end delay, jitter, and control overhead.

The contributions of this work are three-fold:

- A novel routing protocol for FANETs that improves communication performance;
- A weighted metric to account for the stability and quality of links in the forwarding decision;
- A method to determine the best weights for the proposed metric.

The remainder of this work is organized as follows. Section 2 discusses the routing challenge in FANETs. Section 3 presents the related work. Section 4 introduces the proposed routing protocol. The simulated scenario is described in Section 5. Section 6 discusses the assessment results. Finally, Section 7 concludes this paper and presents research directions for future work.

2 Challenges in FANET Routing

Employing Unmanned Aerial Vehicles (UAVs) as network elements poses several challenges that are not common to classic Mobile *Ad-hoc* Networks (MANETs) or Vehicle *Ad-hoc* Networks (VANETs). UAVs have computing and energy constraints and are more susceptible to atmospheric interference. Additionally, the mobility pattern of UAVs differs from the nodes in other *ad-hoc* networks. The UAVs can follow predefined movement patterns or move freely, depending on the application. They also move at medium to high speeds, ranging from 30 to 460 km/h [Lakew *et al.*, 2020]. This is faster than typical nodes in MANETs, which move at around 3 km/h [Eltahir, 2007], and VANETs, in which the speed varies greatly, being limited by roads' maximum speeds [Oubbati *et al.*, 2017]. In cities, speed limits are commonly below 80 km/h. Even on unrestricted highways, a typical car usually does not reach speeds exceeding 200 km/h. Moreover, UAVs move in a three-dimensional space, not restricted by road boundaries. Thus, they can move in any direction at varying altitudes, making movement prediction challenging [Costa *et al.*, 2021], even when UAV movements are predetermined [Lakew *et al.*, 2020].

A FANET is only feasible if there is constant communication between the UAVs [Srivastava and Prakash, 2021]. The communication range between a source node and a destination node can be extended by allowing multi-hop communication between UAVs. In a FANET, at least one of the UAVs can act as a gateway, enabling FANET nodes to communicate with a base station or other physical infrastructure, such as a satellite [Ruiyang *et al.*, 2018; Oubbati *et al.*, 2017]. Connectivity with an external network is interesting because it enables additional services, such as Internet access [Oubbati *et al.*, 2017]. In this context, communication in a FANET can be classified as UAV-to-UAV or UAV-to-Infrastructure. This paper focuses on UAV-to-UAV communication, in which UAVs can communicate in line-of-sight

if obstacles are avoided. Even though line-of-sight favors communication, weather conditions can still interfere.

As any mobile *ad-hoc* network, FANET's topology can change over time. Nevertheless, the changing frequency can be much higher than in classic *ad-hoc* networks due to FANET's characteristics. For instance, topology changes when UAVs fail or enter the network, and links are disrupted by atmospheric interference or changes in UAV positioning. Hence, UAVs are required to be able to reorganize to avoid network partitioning. In the process, UAVs can move in any direction to occupy a new position, complicating movement predictability even when the UAVs are programmed to move as a group in a predetermined way [Lakew *et al.*, 2020]. As a result, link disruptions can become even more frequent, making route convergence a problem. To increase the challenge, UAVs are generally scattered in the sky, and the distance between them can range from hundreds of meters up to one kilometer [Wang *et al.*, 2017]. As a result, the node density in FANETs can vary significantly. Overall, the density in a FANET tends to be much lower than in MANETs and VANETs. As a matter of fact, the FANET's characteristics make routing protocols proposed for MANETs and VANETs unsuitable to be applied in FANETs [Khan *et al.*, 2017].

It is also paramount that routing solutions for FANETs consider mobility models coherent with the nodes' movement in this type of network [Li *et al.*, 2017]. In FANETs, this implies portraying UAVs' speed, direction, and acceleration within a specified region [Hadiwardoyo *et al.*, 2020]. Various mobility models exist for FANETs. The correct application of mobility models in simulated environments aids in deploying FANETs, allowing for better performance prediction. Each mobility model has advantages and disadvantages that can assist in understanding message transmission. Some commonly used mobility models include random, semi-random circular, Gauss-Markov, paparazzi, pheromone-based, and group mobility models [Kaur *et al.*, 2020]. This paper uses the Gauss-Markov mobility model, which captures UAVs' movement patterns' directional persistence and smooth trajectory. The model minimizes sudden movement changes, as it can store the prior direction and speed of a UAV, connecting the previous movements to the upcoming ones [Wheeb *et al.*, 2022].

Routing protocols for FANETs can be categorized as follows: topology-based, location-based, hierarchical, energy-aware, heterogeneous, and bio-inspired. In **topology-based** protocols, routing information must be obtained based on the topological information of nodes before data transmission. In FANETs, these protocols tend to perform poorly due to the frequent topology changes [Oubbati *et al.*, 2017]. **Location-based** protocols route data based on the geographical location of UAVs, attempting to bring the data closer to the destination. Each node determines its own geographical location and makes forwarding decisions based on the destination and neighbors' locations. These protocols are suitable for networks with dynamic topologies, such as FANETs [Khan *et al.*, 2017], as these protocols adapt quickly to topology changes. However, nodes need to use location services, which are usually energy-hungry. **Hierarchical** protocols typically apply an algorithm to divide UAVs into subgroups, referred to as clusters, and then elect a primary UAV, or clus-

ter head, to communicate with nodes in other clusters [Liu *et al.*, 2008]. Such protocols can better cope with the uncertainty of topology and movement in FANETs. However, the cluster heads are single points of failure that can lead to network partitioning in case of failure [Lu *et al.*, 2023]. **Energy-aware** routing protocols focus on energy efficiency to ensure reliable communication and prolonged lifespan of FANETs. Therefore, these protocols are designed to minimize energy consumption in routing tasks to reduce network energy usage [Yang *et al.*, 2021] and extend the lifespan while maintaining communication quality [Baek *et al.*, 2020; Mukherjee *et al.*, 2020]. Most existing routing protocols rely on simplified energy consumption models that may not accurately predict actual energy consumption, reducing routing performance. Additionally, most protocols overlook the challenge of simultaneously considering multiple objectives in practical applications, such as reducing delay and increasing reliability. As the FANET grows in the number of nodes, existing routing protocols may face issues related to low scalability and high complexity [Lu *et al.*, 2023]. **Heterogeneous** routing protocols are typically used when a FANET connects to other networks, such as the cellular network [Sharma *et al.*, 2018]. These protocols often focus on the characteristics of the other networks cooperating with the FANET, which can potentially cause increased latency and energy consumption in the FANET. **Bio-inspired** protocols use models based on natural phenomena to find the best routes [Lakew *et al.*, 2020]. The natural behavior of living beings is mathematically modeled to be employed in several applications, including routing [Li *et al.*, 2018; Lakew *et al.*, 2020]. For instance, the Ant Colony algorithm can be used as a forwarding strategy in a routing-enabled network, considering that the packets (“ants”) will follow the paths with the most “pheromones”, i.e., the path through which most packets are transferred. This type of protocol, however, can be less effective than classic *ad-hoc* network protocols such as AODV [Leonov, 2016]. From the abovementioned categories, the location-based protocols are more suitable for FANETs [Khan *et al.*, 2017] as they adapt quickly to changes in topology despite being highly dependent on accurate information about the nodes’ positions. Therefore, this paper focuses on location-based protocols.

The routing protocols can be proactive or reactive [Younis *et al.*, 2021]. **Proactive** protocols must constantly exchange information between nodes to maintain the routes active regardless of whether the nodes intend to communicate at the moment. All nodes must have updated information about the network’s topology [Shantaf *et al.*, 2020]. Thus, whenever a node wishes to transmit a packet, the routing information is already available in a table due to the pre-registration of routes to all nodes before the data packet transmission [Arnous *et al.*, 2019]. The disadvantage of proactive protocols is the control message overhead required to maintain and update routing tables [Ramphull *et al.*, 2021]. In networks with highly dynamic topologies like FANETs, this overhead becomes even more significant due to frequent link breaks that alter the network’s topology. In contrast to proactive protocols, **reactive** protocols discover routes on-demand, i.e., only when a node wants to transmit a packet to a specific destination. A route discovery process precedes the packet

transmission [Biswas and Dasgupta, 2019]. Reactive protocols result in less control overhead in the network than proactive protocols, but the on-demand calculation can increase end-to-end latency [Liu *et al.*, 2019].

Routing protocols may follow diverse forwarding strategies. For instance, based on prediction, delay tolerance, greedy algorithms, machine learning, beacon usage, among others [Oubbati *et al.*, 2017]. **Prediction-based** strategies consider nodes’ geographical position, direction, and speed to predict future positions. These strategies are heavily impacted when nodes can move in any direction in three-dimensional space [Oubbati *et al.*, 2017], making protocols more complex and less accurate. Consequently, there may be a significant increase in delay due to the need for re-transmissions. The **delay-tolerant** strategies should only be used when the application can tolerate delay since the employed forwarding mechanism, “store-carry-and-forward”, introduces significant delay [Usman *et al.*, 2020]. **Greedy algorithms** always choose the best node to the destination based on the local information, for instance, the node closest to the destination based on the current location of the forwarding node. These algorithms potentially get stuck in a local optimal when no best node to the destination is found, but the current node cannot directly reach the destination [Oubbati *et al.*, 2017]. **Machine learning-based** approaches optimize routing decisions based on various network parameters. Although promising, this strategy can be computationally expensive, increasing memory and processing consumption [Oubbati *et al.*, 2019]. Consequently, there is an increase in the energy consumption of network nodes, which is a limited resource in FANETs. Finally, **beaconless** protocols send data in broadcast to all neighboring nodes, and only one of these nodes forwards the data. Forwarding can be based on the relative position between the current node, source, and destination. This approach ignores some common issues in wireless networks, such as interference, collisions, and packet losses, resulting in the selection of unreliable neighbors as the next hop. Thus, retransmissions increase, leading to higher control overhead and total delay [Kim *et al.*, 2020]. In this paper, increasing the communication delay and the consumption of energy and computational resources are considered detrimental. Therefore, beaconless approaches and those based on machine learning, prediction, and delay tolerance are deemed inappropriate. Considering the existence of simple solutions that avoid the local optimum problem when using greedy algorithms, this paper focuses on a greedy approach.

3 Related Work

GPSR is a classic routing protocol proposed by Karp and Kung, which exploits the correspondence between geographic position and connectivity in wireless networks by using the positions of nodes to make packet forwarding decisions [Karp and Kung, 2000]. GPSR can be categorized as a proactive protocol, as it needs to maintain the information about neighboring nodes’ positions proactively, and also as a reactive protocol, as it does not proactively maintain routes. This protocol is location-based in nature and uses

a greedy forwarding strategy to get closer to the destination progressively. If the current node is the closest to the destination but cannot reach it directly, the protocol recovers by routing packets around the perimeter of the region this node is within. GPSR uses control messages to preserve updated neighbors' geographical information. This protocol usually performs better than other classic *ad-hoc* routing protocols, such as AODV and Optimized Link State Routing (OLSR), in dynamic networks.

Kim et al. introduce topology-based variants of AODV and OLSR for FANETs, adapting them to the specific characteristic of constrained energy in such networks [Kim *et al.*, 2018]. Besides being topology-based, the variants are classified as reactive if based on AODV and proactive if based on OLSR. The authors propose methods to calculate network density and determine if the quantity of UAVs is sufficient for the network to achieve adequate performance levels. The network's quality is assessed based on the successfully transmitted packet rate and data throughput. Using the aforementioned metrics, the interval between `hello` control messages is dynamically adjusted based on the UAVs' speed and the number of UAVs in the network. If the network lacks sufficient UAVs to perform correctly, a feedback mechanism is applied using `hello` control messages. When a UAV receives a control message and responds with another control message confirming connectivity, the time interval between these control messages is updated on the UAV. As such, high-speed UAVs should have smaller intervals between `hello` control messages to quickly reflect changes in the network's topology. Slower UAVs, on the other hand, may have longer intervals, helping to reduce control overhead in the network. When the network is denser, topology changes occur more frequently, and the interval should be shorter. In contrast, when the network is less dense, changes tend to be less frequent, and larger intervals can be used.

Li and Yan propose the Link stability Estimation-based Preemptive Routing (LEPR) protocol, which evolves AODV to prevent link breaks that will occur shortly [Li and Yan, 2017]. LEPR is a reactive protocol that can be considered a hybrid protocol that uses topology and location information. It can also be categorized as a type of prediction-based protocol, as it does not directly predict the future position of nodes, but it uses location information to predict link stability. Link stability is estimated by utilizing the distance between two UAVs, the maximum transmission range, and the difference in distance between the two UAVs considering the last two `hello` control messages. Two methods for packet routing are then applied: (i) reactive route discovery and (ii) semi-proactive route maintenance. AODV's `hello` control messages are modified to include the UAV's location obtained through the Global Positioning System (GPS) to implement the reactive route discovery process. Route Request (RREQ) messages are altered to include the first-hop UAV's identifier and the link stability metric. Packets are transmitted through the route with the highest link stability. The protocol continually monitors link communication quality, and when it detects that a link is about to break, the semi-proactive route maintenance mechanism is activated to calculate which alternative link offers the best stability to continue packet transmission. LEPR reduces control overhead in the

network, a major issue in AODV for FANETs due to constant link breaks caused by network dynamics.

Gankhuyag et al. introduce the Robust And Reliable Predictive (RARP) protocol [Gankhuyag *et al.*, 2017], built upon AODV, and, as such, it is a reactive and topology-based protocol. However, RREQ messages in AODV are modified to include the UAV's location, trajectory, movement, and probability failure, turning RARP into a hybrid protocol that accounts for both topology and location information. In addition, the forwarding strategy can be classified as a type of prediction-based, as it uses geographical position and movement to determine the link lifetime but not the future position of a node. This probability is calculated based on two attributes: (i) UAV information, such as battery level, and (ii) environmental conditions, like rain, wind, or nearby buildings. With these attributes, the algorithm calculates the connection time and the link failure risk between two nodes. Additionally, RARP considers the number of hops in transmission to choose routes with fewer UAVs involved in the transmission, reducing transmission delay and avoiding nodes with a higher likelihood of transmission failures. After route calculation, the transmitting UAV predicts the destination UAV's future position to use directional antennas for transmission. The use of directional antennas increases transmission distance and avoids packet collisions. However, RARP generates many control messages, and there is no mechanism to balance transmission demands to avoid overload on a node.

Mahmud and Cho. introduce the EE HELLO AODV [Mahmud and Cho, 2019], built upon AODV. EE HELLO AODV uses UAV and network parameters to change the interval between exchanged `hello` control messages and the link lifetime to decrease the protocol's energy cost on the UAV, maintaining the original AODV's route creation and maintenance mechanisms. The goal is to reduce network control overhead, which is intrinsically linked to the energy cost of the UAV. This is a reactive hybrid routing protocol, as it is topology-based and energy-aware. High-speed or dense networks will likely have a shorter interval between `hello` control messages. In comparison, low-speed or sparsely populated networks will likely have a longer interval between control messages. The network density is based on the number of UAVs, the region the network covers, and the average transmission distance of UAVs. The link lifetime is defined by $T = I \times H$, where H is the number of failures in receiving `hello` control messages, and I represents the interval between control messages. Thus, EE HELLO AODV has a dynamic link lifetime based on the control message interval. Moreover, when EE HELLO AODV identifies the network as having low density, a feedback mechanism for `hello` control messages is also applied to maximize the chances of UAVs realizing that a link is valid for a short period.

Li and Huang propose the location-based protocol Adaptive Beacon Scheme for Geographic Routing (ABPP), based on GPSR [Li and Huang, 2017] and, as such, it is a greedy protocol. ABPP is also a prediction-based protocol that analyzes UAVs' movement history to try to predict their future positions using the linear regression method. By applying a fuzzy logic system with the prediction error degree as input, the output is the interval between control messages. Adapta-

tion of control messages' intervals can also be replicated to topology-based transmission protocols.

Yang et al. propose the location-based protocol Greedy-based Backup Routing (GBR) as a solution for all *ad-hoc* networks, using GPSR as a route discovery method [Yang et al., 2011] and, as such, it is a greedy protocol. All nodes broadcast periodic control messages containing their location, allowing all nodes to know the positions of their neighbors. RREQ packets are transmitted via GPSR and include the node position, speed, and expected link lifetime. The protocol creates two distinct routing tables: one with the primary route, following the ideal path traced by GPSR, and the other with the backup route for the next transmission hop in case the primary link is lost. However, GBR does not consider the third dimension in node movement, and despite showing promising results in simulations, the analysis is not compared with more widespread protocols recognized in the literature, such as AODV in MANETs or GPSR in VANETs.

Li et al. propose an energy-aware routing protocol that uses a machine learning-based forwarding strategy [Li et al., 2024]. The authors use Reinforcement Learning (RL) to decide hop-by-hop to which neighbor the packet must be forwarded. The state consists of the battery level, the channel gain, the received signal-to-noise ratio (SNR), the forwarding decision of the neighboring UAVs, the hop count, and the one-hop latency. The authors also propose a Deep RL (DRL) version of the protocol to compress the state space in large-scale networks and address state quantization errors for UAVs with high mobility. The authors evaluate their proposal by simulating 20 UAVs communicating in Line-of-Sight (LoS) and moving according to the Gauss-Markov mobility model. Simulation results demonstrate that the proposed schemes reduce the average end-to-end latency and the routing energy consumption compared to the baseline. The major drawback of the RL-based proposal is its complexity. Like any RL-based approach, it does not scale well to high-dimensional state and action spaces. In turn, DRL may require several iterations to achieve good results.

Hosseinzadeh et al. propose a machine learning-based routing scheme that uses Q-learning and an intelligent filtering algorithm to forward packets [Hosseinzadeh et al., 2023]. The filtering algorithm controls the size of the state space, accelerating Q-learning convergence speed. The filtering algorithm also regulates Q-learning parameters for better adaptation to the FANET environment. The authors model the reward function to account for the connection time between nodes, the residual energy, and the link quality based on the reception rate of hello packets. The authors compare their proposal to other RL-based protocols in a simulated environment using NS-2. The results show that the proposed protocol improves energy consumption, packet delivery ratio, end-to-end delay, and network longevity. Nevertheless, the routing overhead increases significantly.

Guo et al. propose a hierarchical machine learning-based protocol that groups nodes into clusters, the Intelligent Clustering Routing Approach (ICRA) [Guo et al., 2023]. It consists of a clustering module, a clustering strategy adjustment module, and a routing module. Each node calculates its own utility in the clustering process to select the cluster head. The clustering adjustment uses reinforcement learning to deter-

mine the optimal clustering strategy according to the current network state, aiming to maintain network topology stability. The routing module introduces inter and intra-cluster routing methods based on the network topology. The results show that ICRA is faster at forming clusters with improved efficiency and consistent topology stability across different scenarios, outperforming the compared protocols regarding energy efficiency and network longevity [Guo et al., 2023]. Nevertheless, hierarchical protocols usually cause extra overhead due to broadcasting cluster head declarations, cluster joining, and leaving messages [Alam and Moh, 2023].

In contrast to the related work discussed, the proposed protocol, GWPRP, uses a cross-layer and greedy approach to forward packets. Moreover, GWPRP considers the three-dimensional mobility of nodes. The protocol is designed to generate low control overhead in the network, aiming to save the battery power of UAVs. Additionally, it avoids forwarding packets to overloaded nodes or nodes with a high error rate in the link layer, aiming to reduce the packet loss rate and transmission delay.

4 GWPRP: Greedy Weighted Perimeter Routing Protocol

GWPRP is a unicast transmission routing protocol that leverages geographical location and incorporates data from both the link and network layers to determine the path to the destination using a greedy forwarding strategy. It is natural that a location-based routing protocol heavily relies on positioning services, such as the Global Positioning System (GPS). Hence, all nodes in the network need to be equipped with a GPS that periodically updates the node position. The forwarding strategy used in GWPRP requires knowledge about the destination position. In this work, we assume that all

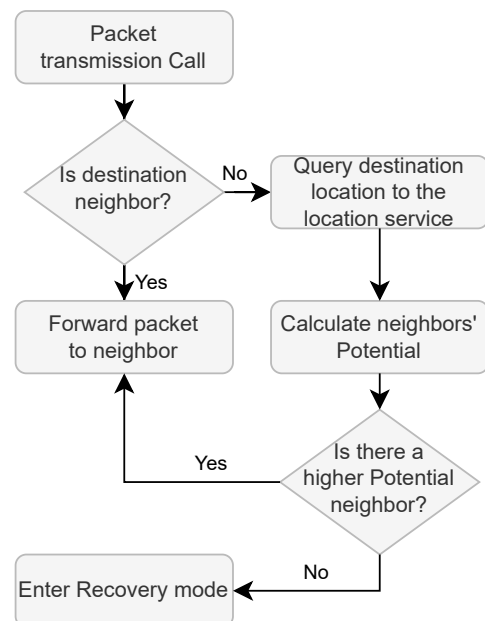


Figure 1. Operation of GWPRP, executed at each hop. Whenever there is a packet to transmit, the destination location is sought, and the Potentials of neighbors are calculated. The packet is forwarded to the neighbor with the highest Potential, which tends to be closest to the destination. The recovery mode is initiated if the algorithm falls into a local optimal.

nodes know such a location. This can be achieved by querying a location service that keeps registers of node positions up to date. The proposed protocol is built upon GPSR but differentiates by considering the (i) three-dimensional location and (ii) cross-layer information in the forwarding decision process. The primary focus of GWPRP is to enhance the packet delivery rate. Thus, it is paramount to have link stability between forwarding nodes, preventing packets from being forwarded to a neighboring node that might have moved beyond the transmission range. Hence, the link stability is accounted for using the number of control messages received from the neighbor node. GWPRP also focuses on simplicity to avoid increasing the end-to-end delay due to excessive processing time, whose increase would lead to higher energy and computing power consumption. Moreover, node reliability is essential, and it is accounted for by modifying the GPSR control messages to include information about the frame error rate in the link layer and the number of packets in the UAV's network layer transmission queue.

GWPRP operates according to the flowchart presented in Figure 1, where the algorithm is executed for each hop and each packet. Whenever the transmitter's network layer receives a transmission request, the protocol asks the location system for the position of the node with the desired IP address. It then calculates the weights of all 1-hop neighbors according to a metric named Potential, proposed in this work. After calculating the neighbors' Potential, GWPRP uses a greedy forwarding heuristic similar to GPSR. The packet is forwarded to the highest Potential neighbor, who is responsible for further forwarding. The neighbor with the highest Potential is the one simultaneously closest to the destination, with the greatest stability in connectivity to the transmitter, lowest occupancy in the transmission queue, and lowest frame error rate. Thus, GWPRP tends to send data to neighbors with the shortest distance to the destination and the highest reliability, considering that reliability depends on the link stability and the node's load. If the current transmitting node has the highest Potential compared to its neighbors, the problem of a local optimal occurs, making it impossible to decide to which neighbor the packet should be forwarded. This can happen when the perceived distance from the neighbor nodes to the destination is longer than from the current nodes. The distance perception is changed by the link quality and link stability considered when the Potential is calculated. Therefore, a node closer to the destination with a bad-quality link will not be used to forward the packet toward the destination. In this case, the protocol activates the Recovery mode, which has two sequential mechanisms to continue the transmission. First, it attempts to identify if there is a node closer to the destination than the current transmitter. If there is no neighbor in this condition, it assumes that there is a straight line connecting the transmitter and the destination. Then, it chooses the neighbor with the smallest angular deviation from the trajectory to the destination node, ignoring the possibility of obstacles such as buildings in the environment. If there is also no neighbor in this situation, the packet is discarded because it is considered impossible to reach the destination.

GWPRP uses three types of information for decision-making regarding the next hop: (i) distance to the destination node, calculated from the location information of the neigh-

bor node received in the control packet and the location of the destination node through the positioning system; (ii) link quality, which is related to the frame error rate and the occupancy of the transmission queue in the network layer of the next hop; and (iii) connectivity stability with each neighbor, determined by the number of hello packets received. The frame error rate is calculated for each node, considering all its links with its neighbors. Considering the number of packets in the queue and the frame error rate, the neighbor selection process for transmission penalizes nodes that are already having difficulty meeting the transmission demand. The number of hello packets, in turn, penalizes nodes that have maintained connectivity with the transmitting node for a short period.

The **Potential** metric aims to identify the neighbor node with the highest probability of successfully transmitting the packet and with the least delay. For each node, the calculation is based on information sent by the neighbor in broadcast hello control packets every 1 second. These packets contain the position (x -, y -, z -axes), frame error rate, and the number of packets the transmitting node has queued in the network layer for transmission. Each node also records the number of hello packets received from each neighbor as an indicator of connectivity stability with the neighbor. The non-receipt of a hello from a neighbor for t seconds implies its removal from the transmitting node's table. Currently, we use $t = 2$. If connectivity with the removed neighbor is re-established, it is treated as a new node. The calculation of the Potential follows Equation 1, where D is the geographic distance between the neighboring node and the destination node, H is the scaled number of hello packets received from the neighbor, Q is the scaled transmission queue occupancy rate in the neighbor's network layer, and FER is the neighbor's frame error rate.

$$Potential = \frac{1}{D \cdot (\delta + \eta \cdot H + \kappa \cdot Q + \phi \cdot FER)} \quad (1)$$

The elements δ , η , κ , and ϕ are multipliers related to the variables D , H , Q , and FER , respectively. GWPRP prioritizes distance as the primary metric, applying the other metrics as a weight for the distance. The idea of this weight is to adjust the perception of the neighbor's distance to the destination observed by the transmitting node, reflecting the link quality in this perception. Thus, the perception of distance is penalized by increasing the perceived distance when link quality is reduced.

The calculation of the multipliers is based on the Analytic Hierarchy Process (AHP) decision-making model, designed to assist in complex decision-making [Darko *et al.*, 2019]. The AHP model divides the overall problem into assessments of lesser importance while simultaneously maintaining the participation of these smaller problems in the global decision. To achieve this, it relativizes the importance of each criterion over other criteria individually. We model the hierarchical structure as follows. The Potential is the overall goal, placed at the first hierarchy level. The group of criteria that relate the options to the goal comprises the Locality, Link Quality, and Link Stability, all placed at the second level. The group of options to achieve this goal is the third level, and

it is composed of distance to the destination, D , frame error rate, FER , scaled transmission queue occupancy, Q , and scaled number of hello packets, H . Option D is related to the Potential via the Locality, Q and FER via the Link Quality, and H via the Link Stability.

Using the AHP model, a judgment matrix is constructed, where columns j and rows i represent criteria at the same level. The elements m_{ij} represent a comparison of importance between pairs of criteria i, j at the same level. The values of the lower triangular matrix are always equal to the inverses of the values of the upper triangular matrix. If $m_{ij} = 1$, criteria i, j have the same importance. If m_{ij} is equal to a value in the set $\{3, 5, 7, 9\}$, criterion i is slightly, moderately, considerably, or significantly more important than criterion j . Values $\{2, 4, 6, 8\}$ for m_{ij} are intermediate. For GWPRP, the judgment matrix is as follows:

$$\begin{array}{c} \text{Loc.} \\ \text{Qual.} \\ \text{Sta.} \end{array} \begin{array}{ccc} \text{Loc.} & \text{Qual.} & \text{Sta.} \\ \begin{pmatrix} 1 & 9 & 9 \\ 1/9 & 1 & 2 \\ 1/9 & 1/2 & 1 \end{pmatrix} \end{array}$$

The main diagonal elements are equal to 1, as a criterion is always equally important to itself. We define the importance of each criterion as follows. The criterion ‘‘Locality’’ ($Loc.$) is represented by the first column or the first row and is significantly more important than all criteria ($m_{12} = m_{13} = 9$). The criterion ‘‘Quality’’ ($Qual.$) is slightly more important than ‘‘Stability’’ ($Sta.$) ($m_{23} = 2$). Thus, the distance is significantly more important than other variables; frame error rate and transmission queue occupancy have the same importance but are slightly less important than the number of hello packets. The values are defined empirically, considering that node location should be more important than other variables, and the consistency index of the judgment matrix should be less than 0.1 for the matrix to be consistent. The consistency index of the constructed matrix is 0.053. The priority of each criterion is calculated through the matrix’s normalized eigenvector. The respective weights of each variable in Equation 1 are equal to the matrix’s eigenvalues following the priority matrix’s columns. For the Link Quality criterion, which has two options, the weight of each option is half of the Link Quality priority. Thus, the weights in Equation 1 are as follows: $\delta = 0.814$, $\phi = 0.057$, $\kappa = 0.057$, and $\eta = 0.072$.

The scaled number of hello packets (H) and the scaled transmission queue occupancy (Q) are discretized before being computed in the Potential. Considering h as the uninterrupted number of hello packets received from the neighbor, f as the limit of omitted hello messages, q as the size of the neighbor’s queue, and c as the capacity of the neighbor’s buffer, Equation 2 shows how the variables H and Q are discretized.

$$H = \begin{cases} 0.5, & \text{if } h = f, \\ 0.25, & \text{if } h > f, \\ 1, & \text{otherwise.} \end{cases} \quad (2)$$

$$Q = \begin{cases} 0.8, & \text{if } q \leq 0.9 \cdot c, \\ 1.1, & \text{otherwise.} \end{cases} \quad (3)$$

It is worth noting that the threshold for the number of hello control messages (h) and the buffer size (q) are parameteriz-

able. In this work, we use $f = 2$, representing two omissions of hello packets and $c = 64$, limiting the buffer size to a maximum of 64 packets. The discretized values for these parameters are obtained empirically.

A higher Potential is obtained when the denominator of Equation 1 is smaller, and therefore, smaller values for D , H , Q , and FER are better. The variable H is related to connectivity stability, so the higher the number of hello packets received, the lower the value of H due to the discretization and the better the stability. Similarly, Q is better when it is smaller, so the number of packets in the transmission queue, q , should occupy the smallest fraction possible of the buffer capacity, c .

Figure 2 illustrates an example of routing with GWPRP. Blue arrows indicate the chosen path at each hop. Each UAV periodically sends hello packets, enabling all UAVs to build or update a list of 1-hop neighbors. When UAV \mathcal{A} wants to send a packet to UAV \mathcal{H} , the routing occurs as follows. \mathcal{A} uses \mathcal{C} to proceed with the transmission. Upon receiving the packet, \mathcal{C} calculates the Potentials of \mathcal{D} and \mathcal{E} . In this example, \mathcal{D} and \mathcal{E} are at the same distance from the destination \mathcal{H} , but \mathcal{E} has a very high number of packets in its transmission queue and a high Frame Error Rate (FER) in the link layer. Suppose that the scaled number of received hello packets $H_{\mathcal{C} \leftarrow \mathcal{D}}$ and $H_{\mathcal{C} \leftarrow \mathcal{E}}$ are equal to 0.25, and the distances $D_{\mathcal{D} \rightarrow \mathcal{H}}$ and $D_{\mathcal{E} \rightarrow \mathcal{H}}$ are equal to 250 m. According to Figure 2 $FER_{\mathcal{D}} = 0.01$, $FER_{\mathcal{E}} = 0.07$, and $Q_{\mathcal{D}} = Q_{\mathcal{E}} = 0.8$. Applying these values to Equation 1 and using the weights obtained from AHP, $Potential_{\mathcal{D}} = 4.6 \times 10^{-3}$ and $Potential_{\mathcal{E}} = 4.5 \times 10^{-3}$. Therefore, the calculated Potential of \mathcal{D} is better than that of \mathcal{E} , and \mathcal{C} decides to send the packet to \mathcal{D} . In turn, \mathcal{D} sends it to \mathcal{F} . As \mathcal{F} has a direct connection to the destination \mathcal{H} , the transmission is done directly.

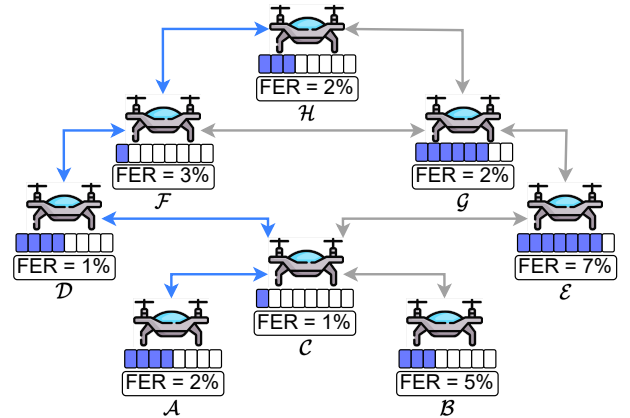


Figure 2. Example of routing in a FANET using GWPRP, between the source \mathcal{A} and the destination \mathcal{H} . At each hop, the Potential is calculated for each neighbor, and the packet is forwarded to the neighbor with the highest Potential. Blue arrows indicate the chosen path at each hop¹.

After calculating the neighbors’ Potentials, GWPRP uses a greedy forwarding heuristic similar to GPSR’s. In the case of GWPRP, the packet is forwarded to the neighbor with the highest Potential. The Recovery mode is initiated if the algorithm does not identify any neighbor with a Potential greater

¹UAV icon, Deus_drone, by Bruce The Deus, Wikimedia Commons, licensed under CC BY-SA 4.0.

than the transmitting node. In this mode, the distance of all neighbors to the destination is calculated in an attempt to continue transmission greedily based only on the distance to the destination node. If no neighbor is better located than the transmitting node, the packet is transmitted to the neighbor that maintains the closest angular trajectory to an imaginary straight line connecting the current transmitter and the destination node. Algorithm 1 shows how the forwarding decision is made at each hop. In lines 6 to 11, the Potential of each neighbor is calculated to find the one with the highest Potential. The packet is forwarded if the neighbor is found, as shown in lines 27 and 28. Otherwise, a local optimal has occurred, and the Recovery process begins, specified in lines 12 to 26, which consists of searching for the neighbor with the shortest geographic distance to the destination (lines 14 to 19) and the smallest angle (lines 20 to 26). At the end of the Recovery process, the packet is discarded if the neighbor is not found, as shown in lines 29 and 30.

Algorithm 1 Forwarding decision-making process.

```

Input: TransmissionRequest
1: highest_potential ← CalculatePotential(tx_node)
2: neighbor ← ∅
3: recovery ← true
4: recovery_angle ← true
5:
6: for i ← 0 to neighbors_list_size do
7:   aux ← CalculatePotential(neighbors_list[i])
8:   if aux > highest_potential then
9:     aux ← highest_potential
10:    recovery ← false
11:    neighbor ← neighbors_list[i]
12: if recovery then
13:   shortest_distance ← CalculateDistanceToDestination(tx_node)
14:   for i ← 0 to neighbors_list_size do
15:     aux ← CalculateDistanceToDestination(neighbors_list[i])
16:     if aux < shortest_distance then
17:       aux ← shortest_distance
18:       recovery_angle ← false
19:       neighbor ← neighbors_list[i]
20:   if recovery_angle then
21:     smallest_angle ← 360
22:     for i ← 0 to neighbors_list_size do
23:       aux ← CalculateAngleToDestination(neighbors_list[i])
24:       if aux < smallest_angle then
25:         aux ← smallest_angle
26:         neighbor ← neighbors_list[i]
27: if neighbor ≠ ∅ then
28:   SendPacket(neighbor)
29: else
30:   DropPacket()

```

5 Simulation Scenario

GWPRP is evaluated through a comparative analysis in a simulated environment using NS-3 version 3.29, a widely used network simulator [Lelio *et al.*, 2020]. The comparison is made with the EE HELLO AODV protocol, based on AODV and designed for FANETs [Mahmud and Cho, 2019], and GPSR. The scenario consists of a network with 40% of nodes acting as sources, 40% as destinations, and 20% of nodes acting only as relays. The idea of this division is to guarantee that the network always has nodes transmitting, receiving, and forwarding packets. The number of nodes varies in the set {30, 40, 50, 60, 70} while maintaining the proportion of source/destination nodes. All nodes have routing capability, and a source node is paired with a single destination node at random. The applications installed on node pairs are grouped

into sets of 4 pairs, and each group transmits at slightly different time instants to avoid collisions at the beginning of the simulation. The applications send data for 120 s at a constant rate of 5 packets/s [Tawfiq *et al.*, 2019]. The packet size varies in the set {64, 128, 256, 512, 1024} B. The nodes move according to the Gauss-Markov mobility model with a constant speed chosen randomly between [18, 144] km/h [Mahmud and Cho, 2019]. The wireless communication standard for each node is IEEE 802.11p [Mallikarachchi *et al.*, 2023], and the transmission radius is 500 m [Mariyappan *et al.*, 2021]. The simulations run 10 times for each combination of protocol, number of nodes, and packet size, changing the random seed to modify movement, initial node placement, and the set of nodes where client and server applications are installed. Propagation loss is modeled considering free-space loss; thus, the Friis propagation loss model is used. The simulations are conducted in a cubic region of 125.000.000 m³. Table 1 summarizes the simulation parameters.

Table 1. Summary of configuration parameters used in the simulation scenario.

Parameter	Value
Initial positioning	Random
Region	125.000.000 m ³
Propagation delay	Constant
Path loss	Friis model
Link and physical layer protocol	IEEE 802.11p
Traffic type	Constant Bit Rate (CBR)
Transport layer protocol	User Datagram Protocol (UDP)
Simulation time	120 seconds
Mobility model	Gauss Markov
Speed	Constant speed randomly chosen from 18 to 144 km/h

6 Results and Discussion

The protocols are compared regarding Packet Delivery Rate (PDR), average end-to-end delay, and average jitter. We also investigate the control overhead by evaluating the number of control packets sent in each simulation. This is important because higher overhead leads to higher energy consumption. Considering the Student's T-distribution, the results are presented with a 95% confidence interval. It is worth noting that the boxplots display both the median (solid line) and the mean (dashed line) in all analyses.

Figure 3 presents the PDR as a function of the number of nodes varying the packet size. The protocol performances are very similar and exhibit closely aligned variability in PDR. On average, GWPRP and EE HELLO AODV show a smaller drop in performance as the number of nodes increases. However, GWPRP tends to be less affected by the increase in packet size compared to others, especially when there are more nodes in the network. Additionally, maintaining the same number of packets but increasing the packet size reduces the delivery rate for all protocols. Considering all results obtained for different numbers of nodes, Figure 3(f) shows that GWPRP tends to have less variability in the de-

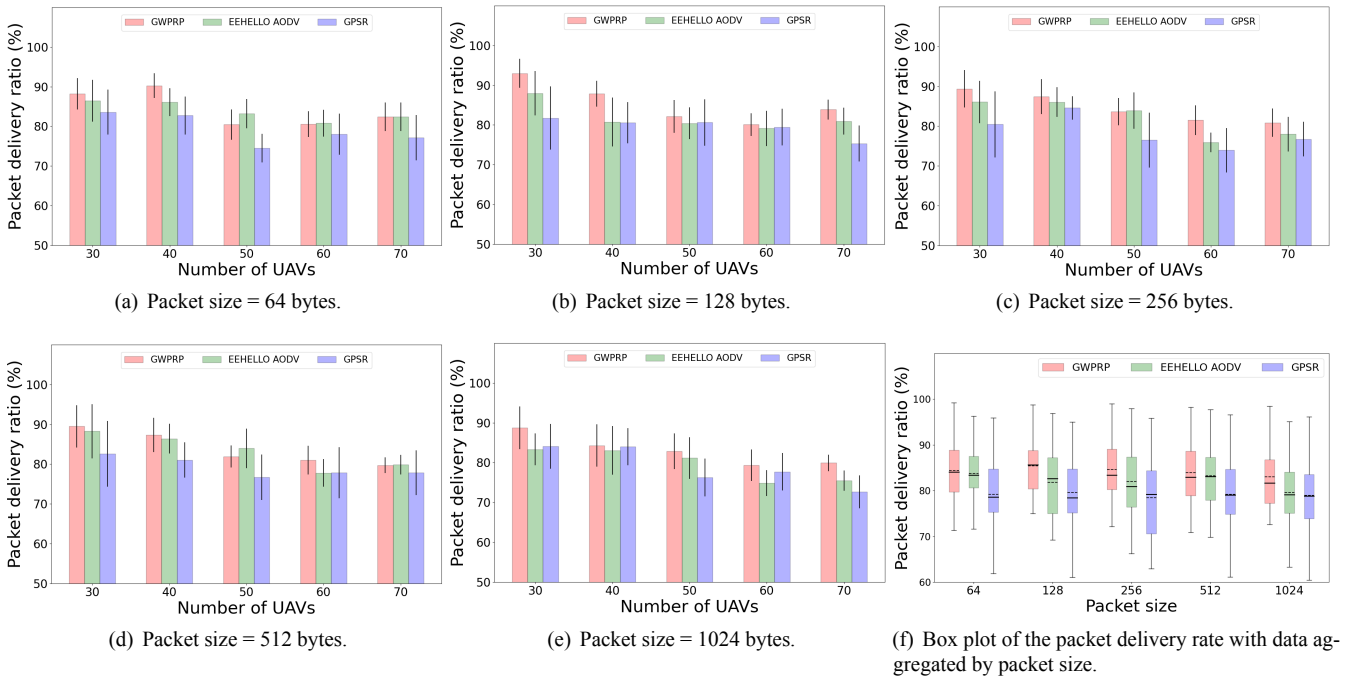


Figure 3. Influence of number of nodes and packet size on the packet delivery ratio. Protocols perform similarly, but GWPRP is less affected by the increase in the packet size and number of nodes.

livery rate and is less affected when the packet size varies. The average delivery rate for GWPRP is around 84%, considering all variations in packet size and number of nodes, while for EE HELLO AODV it is around 82%. GPSR has the lowest average, around 79%.

Figure 4 presents the result for the average end-to-end delay as the number of nodes and packet size vary. GWPRP outperforms EE HELLO AODV in all scenarios and performs similarly to GPSR when packets are smaller than 512 B. When the packet size increases to 1024 B, the average end-to-end delay for GPSR grows exponentially with the network size. Figure 4(f) shows that GWPRP tends to have less variability in the average end-to-end delay when the packet size varies, even considering all results obtained for different numbers of nodes. The average end-to-end delay for GWPRP is around 13 milliseconds, considering all variations in packet size and number of nodes, while EE HELLO AODV has an average of around 27 milliseconds, and GPSR has the worst result, with an average of around 65 milliseconds.

Regarding the average end-to-end jitter, Figure 5 shows the result. EE HELLO AODV has the worst performance among the protocols for packets with a size of 512 B or smaller. For packets with a size of 1024 B, GPSR shows a tendency of exponential growth with the increase in the number of nodes in the network. Figure 5(f) shows that GWPRP tends to have the highest consistent results when the packet size varies, considering all results obtained for different numbers of nodes. The average perceived end-to-end jitter for GWPRP is around 9 milliseconds, considering all variations in packet size and the number of nodes, while GPSR achieves around 65 seconds and EE HELLO AODV, around 22 milliseconds. The significant increase in delay and jitter for GPSR when the packet size is 1024 B and the number of nodes increases may indicate scalability issues for this proto-

col. GWPRP and EE HELLO AODV perform similarly regarding the PDR, but GWPRP achieves significantly lower average end-to-end delay and jitter.

Lastly, we assess the control overhead in each scenario. Figure 6 shows the results. On the one hand, the control overhead is little influenced by the variation in packet size. Hence, the results are shown only for small, medium, and big packets. This result is expected since the number of control messages is independent of the size of the packet, but we can observe a small variation in the number of control messages because bigger packets are more likely than smaller packets to not transfer successfully. As such, new control messages are generated to retry the MAC Layer retransmission, slightly increasing the number of control messages. In the other hand, the number of UAVs can greatly impact the control overhead for all protocols. This is due more control messages being generated because there are more UAVs in the network, and because more UAVs lead to more packets that can suffer interference and collision due to more intense medium contending. Regarding each protocol, it is clear that EE HELLO AODV has much more control overhead than GWPRP and GPSR. This is expected because EE HELLO AODV is a reactive protocol that needs to discover the entire route before sending the packet, but the route may change quickly due to the network dynamics. This causes RERR packets to be more frequent and more RREQs to be generated to find the new route. GWPRP control messages are based on GPSR's and, as such, it is expected to have very similar behavior. We highlight that the energy efficiency of a network is directly related to the effort to send packets. This is especially true for wireless networks, in which changing the radio from idle to active to send the packets increases energy consumption. Therefore, data packets need to be sent with the lowest overhead possible, aiming to minimize the

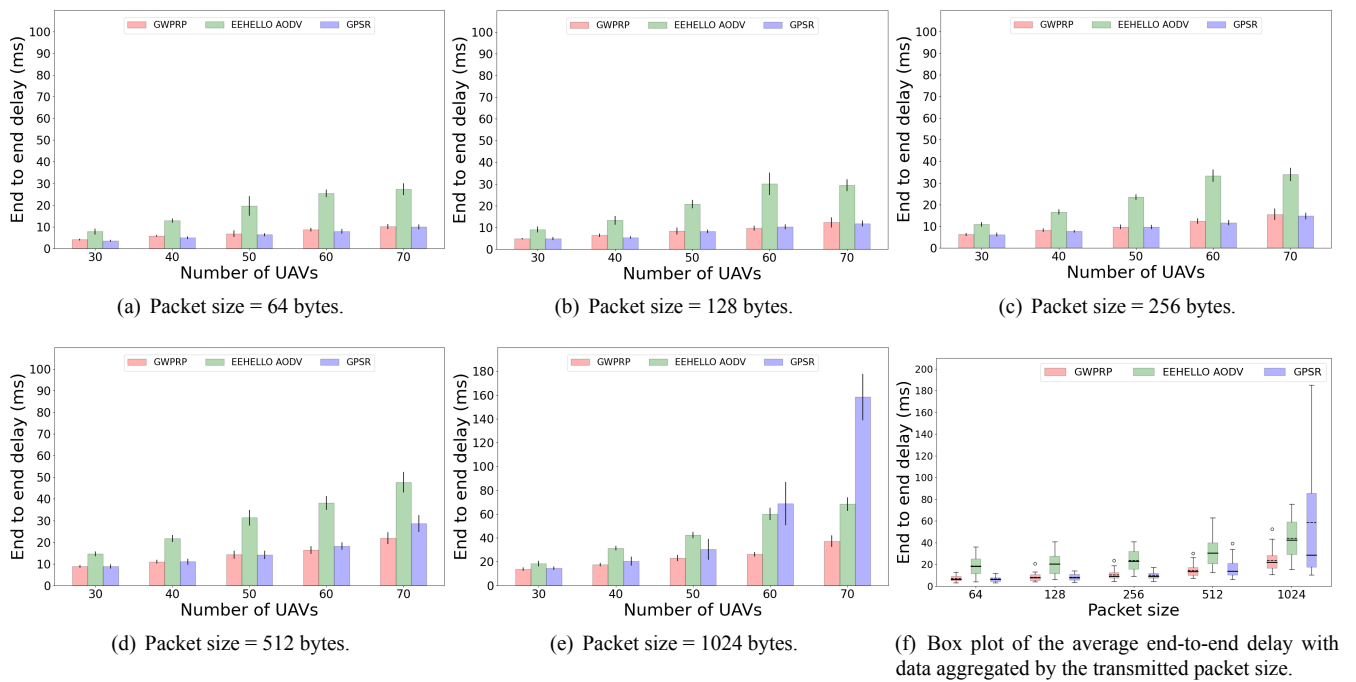


Figure 4. Influence of the number of nodes and packet size on the average end-to-end delay experienced by delivered packets. GPSR performs the worst when the packet size is 1024 B, and the number of nodes increases. GWPRP outperforms both protocols, achieving a much lower average end-to-end delay.

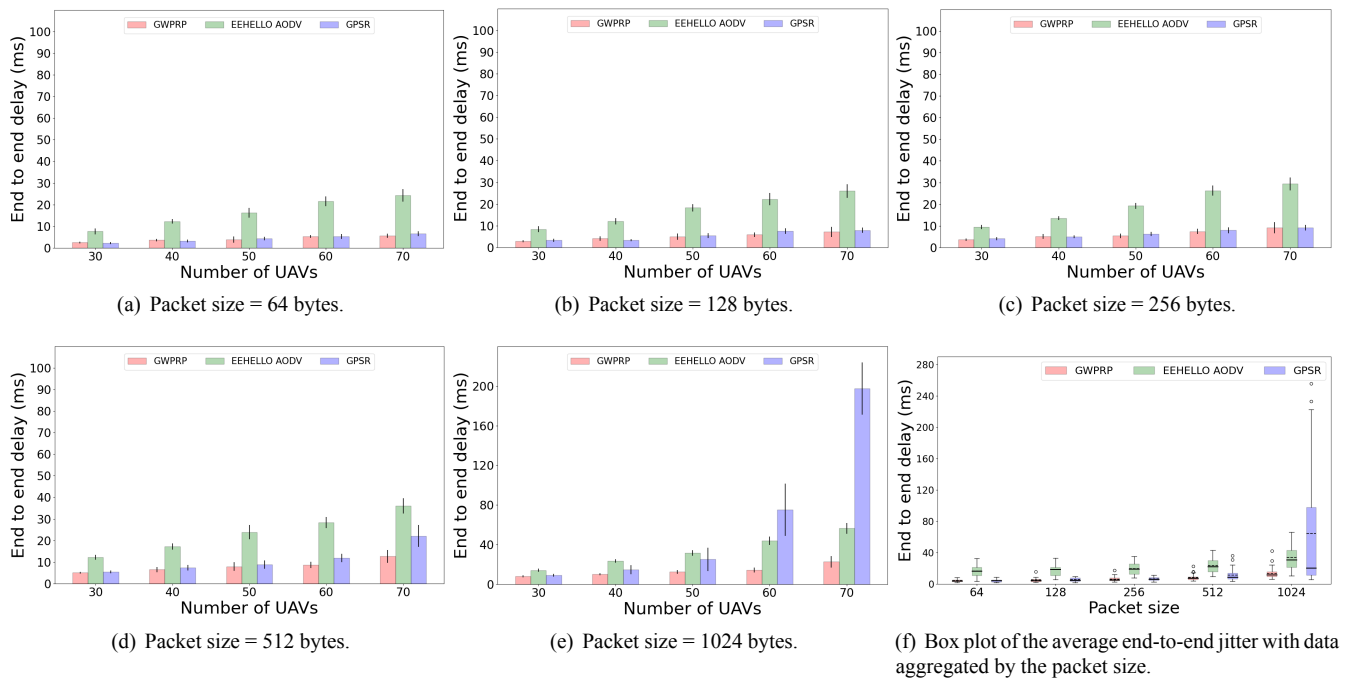


Figure 5. Influence of varying the number of nodes and packet sizes on the jitter experienced by packets.

energy consumed by the network to send the important information. Concerning the energy consumption due to the control overhead to forward packets, GWPRP and GPSR are significantly more efficient than the energy-aware EE HELLO AODV protocol.

The obtained results are consistent with the functioning of the protocols. GWPRP generally shows the best performance, being less affected by network growth. The improved performance observed when increasing the number of nodes in the network indicates that GWPRP tends to be more scalable than the other protocols. GWPRP’s perfor-

mance is considerably better compared to GPSR, especially regarding delay, because GWPRP accounts for the Potential of neighboring nodes, which includes the number of packets in the transmission queue of neighboring nodes, the frame error rate, and the number of exchanged control messages. Additionally, GWPRP considers the three-dimensional mobility of nodes, while GPSR considers only two-dimensional mobility, which may lead to the misplacement of nodes, considering distant nodes in height as neighbor nodes. Compared to EE HELLO AODV, the results tend to be better because EE HELLO AODV introduces a significant delay

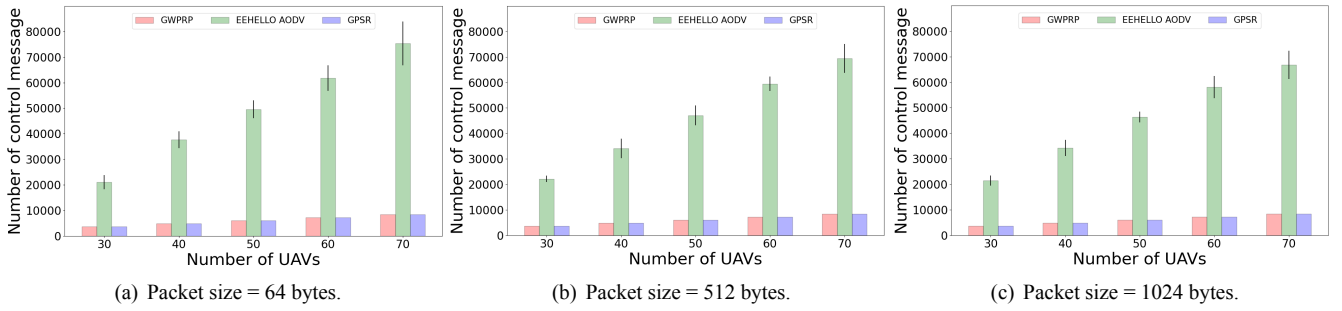


Figure 6. Influence of varying the number of nodes and packet sizes on the control overhead.

component due to the route discovery process using Route Request (RREQ) and Route Reply (RREP) messages. Additionally, the high speed of nodes implies frequent changes in the network topology, increasing the number of times the route discovery process must be executed, resulting in the higher control overhead and average end-to-end delay and jitter observed in the simulations. It is important to highlight that achieving smaller control overhead, while delivering more data packets successfully is critical in a FANET as it means that UAVs spend less energy per successfully transmitted packet.

6.1 Protocol Limitations

The evaluation of the proposed routing protocol is performed in a scenario where the mobility model follows a semi-random pattern, which is dependent on the previous state of the node. Updates for the node speed and direction depend on a Gaussian-distributed random variable. In addition, the propagation loss is modeled by the free-space loss model, following the Friis equation. As such, multipath and obstructions are not taken into account. The evaluation scenario influences directly the results, as it is a simplification of reality. The proposed protocol heavily relies on the Potential metric to identify the next hop toward the destination. The Potential considers the geographic distance between the neighboring nodes and the destination node, D , the scaled number of hello packets received from the neighboring nodes, H , the scaled transmission queue occupancy rate in the neighboring nodes' network layer, Q , and the frame error rate of neighboring nodes, FER . Different mobility and propagation loss models can affect directly all these variables. For instance, if we take into account multipath fading via the introduction of the Nakagami model and shadowing effects via the Log-Distance model, the link quality would be worsened, reducing the number of hello packets, probably increasing the queue occupancy rate in the network layer, and increasing the frame error rate. Hence, we would see increased H , increased Q , and increased FER . As a consequence, the Potential for nodes in propagation-impaired locations would be reduced. This can modify the routes chosen by GWPRP, but it is not possible to state that these routes would result in higher delays. On one hand, it is expected that the packet delivery ratio will decrease. On the other hand, the competing protocols will also suffer, resulting in a decrease in the packet delivery ratio. As these protocols do not take into account the link quality, the packet delivery ratio should be lower com-

pared to GWPRP, but EE HELLO AODV will probably have a slightly lesser reduction, as it accounts for link lifetime.

Even though GWPRP accounts for link quality and stability, the non-deterministic influence of propagation conditions can pose a problem. Such influence can make the Potential of adjacent nodes change quite randomly, which can incur in loops. Nevertheless, it is possible to use the Recovery Mode, developed to avoid the local minimum problem, to break loops. For instance, if the node can count how many times the same packet has been seen and forwarded, it is possible to set a count threshold, from which the node enters the Recovery Mode, using the distance and angle properties to forward the packet.

Due to the nature of the protocol, it depends on accurate position information that, in turn, depends on well-functioning GPS. High precision GPS should be used to lower localization errors. The location service is essential for position-based protocols and frequent position updates should happen to keep nodes' positions up to date, resulting in high energy consumption, especially in highly dynamic networks. The use of beacons also impacts energy consumption negatively. As such, a beaconless version of GWPRP may improve energy efficiency at the cost of increasing communication delay.

The Gauss-Markov mobility model results in smoother movement patterns, as it maintains the correlation between the speed and direction of successive states. As it introduces limited randomness, rapid movement changes are not captured by this model. Hence, it is important to highlight that the smoother movement can inflate the packet delivery ratio compared to real scenarios, as it can mask the frequency of link breakages. More stable links can also influence end-to-end delay and jitter, reducing these metrics, and the routing overhead, reducing the number of control packets. Nevertheless, the choice of mobility model benefits all protocols evaluated in this work. Concerning location-based protocols such as GPSR and GWPRP, the Gauss-Markov model can lead to an optimistic result due to fewer occurrences of local minimum, resulting from more stable links. As such, erratic models, such as the random waypoint, can be used to evaluate the protocols' performances in scenarios where drastic changes in the movement pattern are expected.

7 Conclusion

Using multiple UAVs to build FANETs simplifies task execution and enhances network resilience but introduces a dynamically changing topology in which routing is challenging. This paper proposed the GWPRP, a cross-layer location-based protocol that employs a greedy forwarding strategy to select the next hop on the path to the destination. GWPRP is an evolution of GPSR, a classic location-based protocol that also uses a greedy strategy. Unlike GPSR, GWPRP considers the frame error rate at the link layer and the transmission queue occupancy at the network layer of neighboring nodes to determine link quality. It also considers the number of control messages exchanged with the neighbors to determine link stability. Based on this information, the Potential of each neighbor is calculated, indicating which neighbor has links with higher quality and stability and is closer to the destination. Thus, GWPRP tends to forward packets towards the destination using more stable and higher-quality links. The proposed protocol was evaluated through simulations in NS-3 in a scenario where nodes move freely in three dimensions, following a Gauss-Markov mobility model. The number of nodes and the packet size vary to assess the impact on the performance of three routing protocols: GWPRP, EE HELLO AODV, and GPSR. The results showed that the GWPRP achieved a packet delivery ratio similar to the other protocols but with a slightly higher average and lower impact of packet and network sizes. GWPRP has a lower average end-to-end delay and jitter. The control overhead is also smaller for GWPRP, compared to EE HELLO AODV, due to the nature of the protocols. The results indicate that GWPRP outperforms the other protocols, being more scalable and spending less energy, as the control overhead is smaller and the packet delivery ratio is higher. Future work for this research includes improvements to GWPRP, such as determining link stability based on contact time prediction and using dynamic periodicity for control message transmission based on relative node speed. Finally, efforts are planned to assess the energy impact of the proposed protocol directly.

Declarations

Funding

This research was partially funded by CNPq, CAPES, FAPERJ, RNP and Niterói City Hall.

Authors' Contributions

Rian Moreira performed the experiments, validation, and visualization of this work. Rian Moreira wrote the original draft of this work. Dianne Medeiros contributed to this work's conception, methodology, and supervision. Dianne Medeiros reviewed and edited the manuscript. All authors read and approved the final manuscript.

Competing interests

The authors declare that they have no competing interests.

Availability of data and materials

The module for NS-3 version 3.29 developed in this work is available on <https://github.com/rdias612/GWPRP-ns3.29>.

References

- A. Chrikiac, H. Touatia, H. S. and Kamoun, F. (2019). FANET: Communication, mobility models and security issues. *Computer Networks*, 163. DOI: 10.1016/j.comnet.2019.106877.
- Alam, M. M. and Moh, S. (2023). Q-learning-based routing inspired by adaptive flocking control for collaborative unmanned aerial vehicle swarms. *Vehicular Communications*, 40:100572. DOI: <https://doi.org/10.1016/j.vehcom.2023.100572>.
- Arnous, R., El-kenawy, E.-S., and Saber, M. (2019). A proposed routing protocol for mobile ad hoc networks. *International Journal of Computer Applications*, 178:26–30. DOI: 10.5120/ijca2019919305.
- Ashish, S. and Jay, P. (2021). Future FANET with application and enabling techniques: Anatomization and sustainability issues. *Computer Science Review*, 39. DOI: 10.1016/j.cosrev.2020.100359.
- Baek, J., Han, S. I., and Han, Y. (2020). Energy-efficient uav routing for wireless sensor networks. *IEEE Transactions on Vehicular Technology*, 69(2):1741–1750. DOI: 10.1109/TVT.2019.2959808.
- Biswas, A. and Dasgupta, M. (2019). AODV-DSR hybrid reactive routing protocol and its generalization for mobile ad-hoc networks. In *2019 3rd International Conference on Electronics, Materials Engineering & Nano-Technology (IEMENTech)*, pages 1–5. DOI: 10.1109/IEMENTech48150.2019.8981052.
- Costa, L., Kunst, R., and de Freitas, E. (2021). Q-FANET: Improved Q-learning based routing protocol for FANETs. *Computer Networks*, 198. DOI: 10.1016/j.comnet.2021.108379.
- Darko, A., Chan, A., E.E. Ameyaw, E. O., Pärn, E., and Edwards, D. (2019). Review of application of analytic hierarchy process (AHP) in construction. *International Journal of Construction Management*. DOI: 10.1080/15623599.2018.1452098.
- Eltahir, I. (2007). The impact of different radio propagation models for mobile ad hoc networks (MANET) in urban area environment. In *The 2nd International Conference on Wireless Broadband and Ultra Wideband Communications (AusWireless 2007)*, pages 30–30. DOI: 10.1109/AUSWIRELESS.2007.80.
- Gankhuyag, G., Shrestha, A., and Yoo, S.-J. (2017). Robust and reliable predictive routing strategy for flying ad-hoc networks. *IEEE Access*, 5:643–654. DOI: 10.1109/ACCESS.2017.2647817.
- Guo, J., Gao, H., Liu, Z., Huang, F., Zhang, J., Li, X., and Ma, J. (2023). ICRA: An intelligent clustering routing approach for uav ad hoc networks. *IEEE Transactions on Intelligent Transportation Systems*, 24(2):2447–2460. DOI: 10.1109/TITS.2022.3145857.
- Hadiwardoyo, S. A., Dricot, J.-M., Calafate, C. T., Cano, J.-

- C., Hernández-Orallo, E., and Manzoni, P. (2020). UAV mobility model for dynamic UAV-to-car communications in 3D environments. *Ad Hoc Networks*, 107:102193. DOI: 10.1016/j.adhoc.2020.102193.
- Hosseinzadeh, M., Ali, S., Ionescu-Feleaga, L., Ionescu, B.-S., Yousefpoor, M. S., Yousefpoor, E., Ahmed, O. H., Rahmani, A. M., and Mehmood, A. (2023). A novel Q-learning-based routing scheme using an intelligent filtering algorithm for flying ad hoc networks (FANETs). *Journal of King Saud University - Computer and Information Sciences*, 35(10):101817. DOI: <https://doi.org/10.1016/j.jksuci.2023.101817>.
- Karp, B. and Kung, H. (2000). GPSR: greedy perimeter stateless routing for wireless networks. In *Proceedings of the 6th annual international conference on Mobile computing and networking*. DOI: 10.1145/345910.345953.
- Kaur, P., Singh, A., and Gill, S. S. (2020). Rgim: An integrated approach to improve qos in aodv, dsr and dsdv routing protocols for fanets using the chain mobility model. *The Computer Journal*, 63. DOI: 10.1093/comjnl/bxaa040.
- Khan, F., Yau, K.-L., Md. Noor, R., and Imran, M. (2019). Routing schemes in fanets: A survey. *Sensors (Basel, Switzerland)*, 20. DOI: 10.3390/s20010038.
- Khan, M., Qureshi, I., Safi, A., and Khan, I. (2017). Flying ad-hoc networks (FANETs): A review of communication architectures, and routing protocols. In *2017 First International Conference on Latest trends in Electrical Engineering and Computing Technologies (INTELLECT)*. DOI: 10.1109/INTELLECT.2017.8277614.
- Khan, S. K., Naseem, U., Siraj, H., Razzak, I., and Imran, M. (2021). The role of unmanned aerial vehicles and mmWave in 5G: Recent advances and challenges. *Transactions on Emerging Telecommunications Technologies*, 32(7):e4241. DOI: <https://doi.org/10.1002/ett.4241>.
- Kim, B.-S., Ullah, S., Kim, K. H., Roh, B., Ham, J.-H., and Kim, K.-I. (2020). An enhanced geographical routing protocol based on multi-criteria decision making method in mobile ad-hoc networks. *Ad Hoc Networks*, 103:102157. DOI: <https://doi.org/10.1016/j.adhoc.2020.102157>.
- Kim, G.-H., Mahmud, I., and Cho, Y.-Z. (2018). Hello-message transmission-power control for network self-recovery in FANETs. In *2018 Tenth International Conference on Ubiquitous and Future Networks (ICUFN)*, pages 546–548. DOI: 10.1109/ICUFN.2018.8436645.
- Lakew, D., Sa'ad, U., Dao, N.-N., Na, W., and Cho, S. (2020). Routing in flying ad hoc networks: A comprehensive survey. *IEEE Communications Surveys & Tutorials*, PP:1–1. DOI: 10.1109/COMST.2020.2982452.
- Lelio, C., Marco, G., Mauro, I., Fiammetta, M., and Michele, M. (2020). Computer network simulation with ns-3: A systematic literature review. *Electronics*. DOI: 10.3390/electronics9020272.
- Leonov, A. V. (2016). Application of bee colony algorithm for fanet routing. In *2016 17th International Conference of Young Specialists on Micro/Nanotechnologies and Electron Devices (EDM)*, pages 124–132, Erlagol, Russia. IEEE. DOI: 10.1109/EDM.2016.7538709.
- Li, J., Xiao, L., Qi, X., Lv, Z., Chen, Q., and Liu, Y.-J. (2024). Reinforcement learning based energy-efficient fast routing for FANETs. *IEEE Transactions on Communications*, pages 1–1. DOI: 10.1109/TCOMM.2024.3409561.
- Li, X. and Huang, J. (2017). ABPP: An adaptive beacon scheme for geographic routing in FANET. *18th International Conference on Parallel and Distributed Computing, Applications and Technologies*. DOI: 10.1109/PD-CAT.2017.00055.
- Li, X., Keegan, B., and Mtenzi, F. (2018). Energy efficient hybrid routing protocol based on the artificial fish swarm algorithm and ant colony optimisation for WSNs. *Sensors*, 18:3351. DOI: 10.3390/s18103351.
- Li, X. and Yan, J. (2017). LEPR: Link stability estimation-based preemptive routing protocol for flying ad hoc networks. In *IEEE Symposium on Computers and Communications*. DOI: 10.1109/ISCC.2017.8024669.
- Li, X., Zhang, T., and Li, J. (2017). A particle swarm mobility model for flying ad hoc networks. In *GLOBECOM 2017 - 2017 IEEE Global Communications Conference*, pages 1–6. DOI: 10.1109/GLOCOM.2017.8253966.
- Liu, J., Wang, Q., He, C., Jaffres-Runser, K., Xu, Y., Li, Z., and Xu, Y.-J. (2019). Qmr:q-learning based multi-objective optimization routing protocol for flying ad hoc networks. *Computer Communications*, 150. DOI: 10.1016/j.comcom.2019.11.011.
- Liu, K., Zhang, J., and Zhang, T. (2008). The clustering algorithm of UAV networking in near-space. In *2008 8th International Symposium on Antennas, Propagation and EM Theory*, pages 1550–1553, Kunming, China. IEEE. DOI: 10.1109/ISAPE.2008.4735528.
- Lu, Y., Wen, W., Igorevich, K., Ren, P., Zhang, H., Duan, Y., Zhu, H., and Zhang, P. (2023). Uav ad hoc network routing algorithms in space-air-ground integrated networks: Challenges and directions. *Drones*, 7:448. DOI: 10.3390/drones7070448.
- Mahmud, I. and Cho, Y.-Z. (2019). Adaptive hello interval in FANET routing protocols for green UAVs. *IEEE Access*, 7:63004–63015. DOI: 10.1109/ACCESS.2019.2917075.
- Mallikarachchi, D., Wong, K., and Lim, J. M.-Y. (2023). An authentication scheme for fanet packet payload using data hiding. *Journal of Information Security and Applications*, 77:103559. DOI: <https://doi.org/10.1016/j.jisa.2023.103559>.
- Mariyappan, K., Christo, M. S., and Khilar, R. (2021). Implementation of fanet energy efficient aodv routing protocols for flying ad hoc networks [FEEAODV]. *Materials Today: Proceedings*. DOI: 10.1016/j.matpr.2021.02.673.
- Mukherjee, A., Misra, S., Chandra, V. S. P., and Raghuwanishi, N. S. (2020). Ecor: Energy-aware collaborative routing for task offload in sustainable uav swarms. *IEEE Transactions on Sustainable Computing*, 5(4):514–525. DOI: 10.1109/TSUSC.2020.2976453.
- Oubbati, O., Lakas, A., f. Zhou, and Güneş, M. (2017). A survey on position-based routing protocols for flying ad hoc networks (FANETs). *Vehicular Communications*, 10:29–56. DOI: 10.1016/j.vehcom.2017.10.003.
- Oubbati, O. S., Atiquzzaman, M., Lorenz, P., Tareque, M. H., and Hossain, M. S. (2019). Routing in flying ad hoc networks: Survey, constraints, and future challenge perspec-

- tives. *IEEE Access*, 7:81057–81105. DOI: 10.1109/ACCESS.2019.2923840.
- Ramphull, D., Mungur, A., Armoogum, S., and Pudaruth, S. (2021). A review of mobile ad hoc network (manet) protocols and their applications. In *2021 5th International Conference on Intelligent Computing and Control Systems (ICICCS)*, pages 204–211. DOI: 10.1109/ICICCS51141.2021.9432258.
- Ruiyang, D., Wang, J., Jiang, C., Ren, Y., and Hanzo, L. (2018). The transmit-energy vs computation-delay trade-off in gateway-selection for heterogenous cloud aided multi-uav systems. *IEEE Transactions on Communications*, PP:1–1. DOI: 10.1109/TCOMM.2018.2889672.
- Shantaf, A. M., Kurnaz, S., and Mohammed, A. H. (2020). Performance evaluation of three mobile ad hoc network routing protocols in different environments. In *2020 International Congress on Human-Computer Interaction, Optimization and Robotic Applications (HORA)*, pages 1–6, Ankara, Turkey. IEEE. DOI: 10.1109/HORA49412.2020.9152845.
- Sharma, V., Kumar, R., and Kumar, N. (2018). Dptr: Distributed priority tree-based routing protocol for fanets. *Computer Communications*, 122:129–151. DOI: <https://doi.org/10.1016/j.comcom.2018.03.002>.
- Srivastava, A. and Prakash, J. (2021). Future fanet with application and enabling techniques: Anatomization and sustainability issues. *Computer Science Review*, 39:100359. DOI: 10.1016/j.cosrev.2020.100359.
- Tawfiq, N., Lehsaini, M., and Fouchal, H. (2019). Partial backwards routing protocol for VANETs. *Vehicular Communications*, 18:100162. DOI: 10.1016/j.vehcom.2019.100162.
- Usman, Q., Chughtai, O., Nawaz, N., Kaleem, Z., Khaliq, K. A., and Nguyen, L. D. (2020). Lifetime improvement through suitable next hop nodes using forwarding angle in fanet. In *2020 4th International Conference on Recent Advances in Signal Processing, Telecommunications & Computing (SigTelCom)*, pages 50–55. DOI: 10.1109/SigTelCom49868.2020.9199025.
- Wang, J., Jiang, C., Han, Z., Ren, Y., Maunder, R., and Hanzo, L. (2017). Taking drones to the next level: Cooperative distributed unmanned-aerial-vehicular networks for small and mini drones. *IEEE Vehicular Technology Magazine*, 12:73–82. DOI: 10.1109/MVT.2016.2645481.
- Wheeb, A. H., Nordin, R., Samah, A. A., Alsharif, M. H., and Khan, M. A. (2022). Topology-based routing protocols and mobility models for flying ad hoc networks: A contemporary review and future research directions. *Drones*, 6(1). DOI: 10.3390/drones6010009.
- Yang, W., Yang, X., Yang, S., and Yang, D. (2011). A greedy-based stable multi-path routing protocol in mobile ad hoc networks. *Ad Hoc Networks*, 9:662–674. DOI: 10.1016/j.adhoc.2010.09.004.
- Yang, Z., Liu, H., Chen, Y., Zhu, X., Ning, Y., and Zhu, W. (2021). Uee-rpl: A uav-based energy efficient routing for internet of things. *IEEE Transactions on Green Communications and Networking*, 5(3):1333–1344. DOI: 10.1109/TGCN.2021.3085897.
- Younis, Z., Mohsin Abdulazeez, A., Zeebaree, S., Zebari, R., and Zeebaree, Q. (2021). Mobile ad hoc network in disaster area network scenario a review on routing protocols. *International Journal of Online and Biomedical Engineering (iJOE)*, 17:49–75. DOI: 10.3991/ijoe.v17i03.16039.